Journal of Sound and Vibration (1999) **228**(4), 889–914
Article No. jsvi.1999.2455, available online at http://www.idealibrary.com on IDEAL®

MATHEMATICAL MODELLING AND SIMULATION OF VIBRATION CONTROL RESPONSE OF INTERMEDIATE SUPPORT PARAMETERS IN A HANGING CANTILEVER

M. M. Nazeer, A. F. Khan and M. Afzal

Dr. A. Q. Khan Research Laboratories, P.O. Box 502, *Rawalpindi, Pakistan*

AND

N. Ahmed

Mathematics Department, Quaid-i-Azam University, Islamabad, Pakistan

(*Received* 16 *September* 1998, *and in final form* 11 *June* 1999)

Randomly excited vibrations in a vertically hanging cantilever can be damped and controlled by an intermediate support comprising a support tube and an annular ring holding the cantilever at the bottom of the tube. A number of parameters like length and stiffness of the support tube, stiffness of the annular ring, mounting position of the ring with respect to cantilever end and nature of the support provided by the ring may affect the damping in the system. In this work, a mathematical model is developed to simulate the system in order to see the role of these parameters in damping and controlling the vibrations of the cantilever. The computed results for an experimental set-up are discussed and analyzed to elaborate the response of support tube parameters and stiffness of the annular ring. It is observed that knowing the possible range of perturbation frequency and amplitude, the intermediate support parameters can be adjusted to successfully overcome the vibration problem.

1. INTRODUCTION

A long vertically hanging cantilever is always prone to oscillations whenever disturbed by an earthquake or when it experiences an intermittent high-pressure or high-speed fluid flow perturbations. The effect becomes devastating when such a cantilever is in the vicinity of a member moving or rotating at an ultrahigh speed, where a small disturbance reduces the micro clearance between the relatively moving surfaces to zero and hence destabilizes the whole system. One such example is that of a gas feed system comprising a set of vertically hanging tubes rigidly mounted at their top. Their bottom ends are free to oscillate within an ultrahigh-speed rotating cylinder under any external or internal disturbance. Impacts of various flows and machine parameters on vibration of these tubes leading to machine crash were studied in reference [1]. The idea of control of these vibrations by magnet pairs of similar and opposite polarities was discussed in

0022-460X/99/490889 + 26 $30.00/0

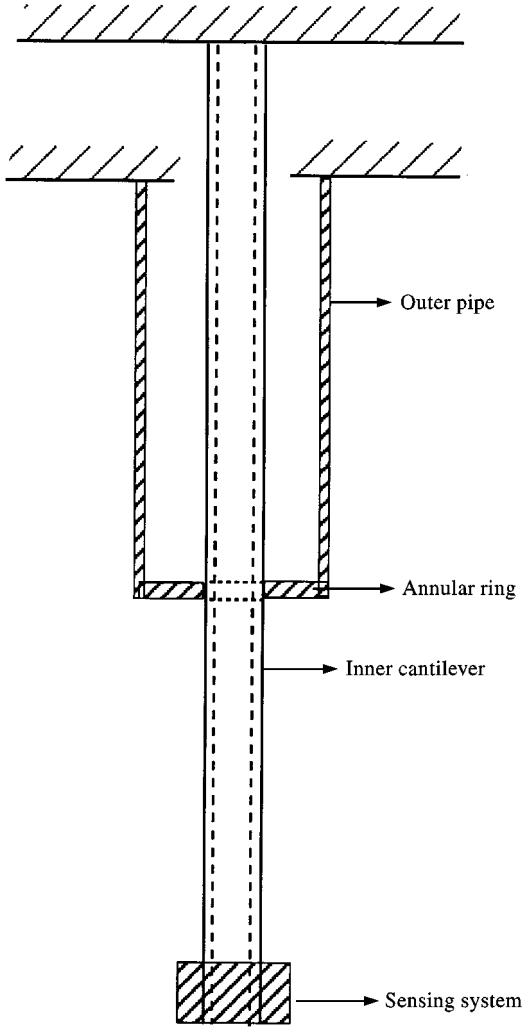

Figure 1. Cantilever with intermediate support.

references [2, 3]. In reference [4], damping achieved experimentally with the help of a loose spring skirting the tube was analyzed. Its mathematical model, computer simulations and detailed analyses of simulated and experimentally observed results of various parameters were presented in references [5–9]. In the present work, the vibration response of the system (Figure 1) having no spring is studied with regard to mechanical and geometrical properties of its components. The system is composed of two concentric tubes having variable lengths, rigidly fixed at their top at different levels. The inner tube extends beyond the outer support tube which constrains it with the help of an annular ring at its bottom end. This will increase the rigidity of the inner tube and protect it from devastation of flow-induced and earthquake-excited oscillations by limiting its vibration amplitude. Factors such as length and thickness of the outer tube, the stiffness of the annular ring and its

position along the length of the inner tube affect the vibration response of the whole system.

The change in flexural stiffness (EI) due to variation in one or more properties like cross-sectional area, shape, orientation with respect to the particular set of axis, material properties or attachments make the system very complex. Change in any of these quantities with the length forms a new segment and thus the total length of the cantilever is divided into a number of segments each having constant properties over the segment length. The segments are numbered from bottom to top, while the impressed force axis is in the horizontal plane and the local and global Z-axes are collinear and point downwards to the bottom end of the lever as shown in Figure 2. Global origin is at the top, i.e., at the fixed end of the cantilever and local origin of a segment is at its own upper end. Viscous damping of the system is intentionally ignored to clearly see the undamped response of the model and its parameters. The longitudinal vibrations and lateral effect of weight of suspended masses in the displaced position on bending and detailed analysis of response of higher mode shapes are deferred presently for simplicity. Also, only the end excitation to give end displacement is considered for the time being and the rest, i.e., multi-point and distributed loads are deferred for subsequent work.

2. MULTI-LINK MULTI-SEGMENT CANTILEVER

The system under study is composed of two concentric tubes with sizable annular clearance and rigid supports at their top end at relatively different heights. The inner thinner tube projects beyond the outer (Figure 1) and is exposed to intermittent vibration exciting force. The two tubes are coupled together at the bottom end of the shorter outer tube with the help of an annular ring of flexible material to minimize the vibration amplitude of the inner tube. The outer and inner tubes may have multi-segments depending upon second moment of area, material properties or attachments. The system may be represented by multi-link multi-segment cantilever with two-dimensional line diagram shown in Figure 2. The links are denoted by W_m, where m refers to the link number.

The deflection at a point in a beam is given by the equation [10–12]

$$y'' = \frac{\mathrm{d}^2 y}{\mathrm{d}z^2} = \frac{M^*}{EI} = \frac{(L - z)F + M'}{EI}, \tag{1}$$

where M^* is the overall bending moment at the point, being sum of M', the pure bending moment exerted at the end of the beam, and due to bending force, F acting at a distance $L - z$ from the point. Here EI is the flexural rigidity of the cross-section of the beam at that point. Let, in general, the mth link of the cantilever be of n segments, numbered from bottom to the top and the system of co-ordinates be local for each segment, such that its origin is at the top of the respective segment, z in downward direction along the cantilever length, x and y in the radial direction passing through the center of the lever perpendicular to each other and parallel to the global set of X- and Y-axes as shown in Figure 2. Thus, the global X-axis and all the local x-axes are coplanar and parallel to exciting force F_x and global Y-axis,

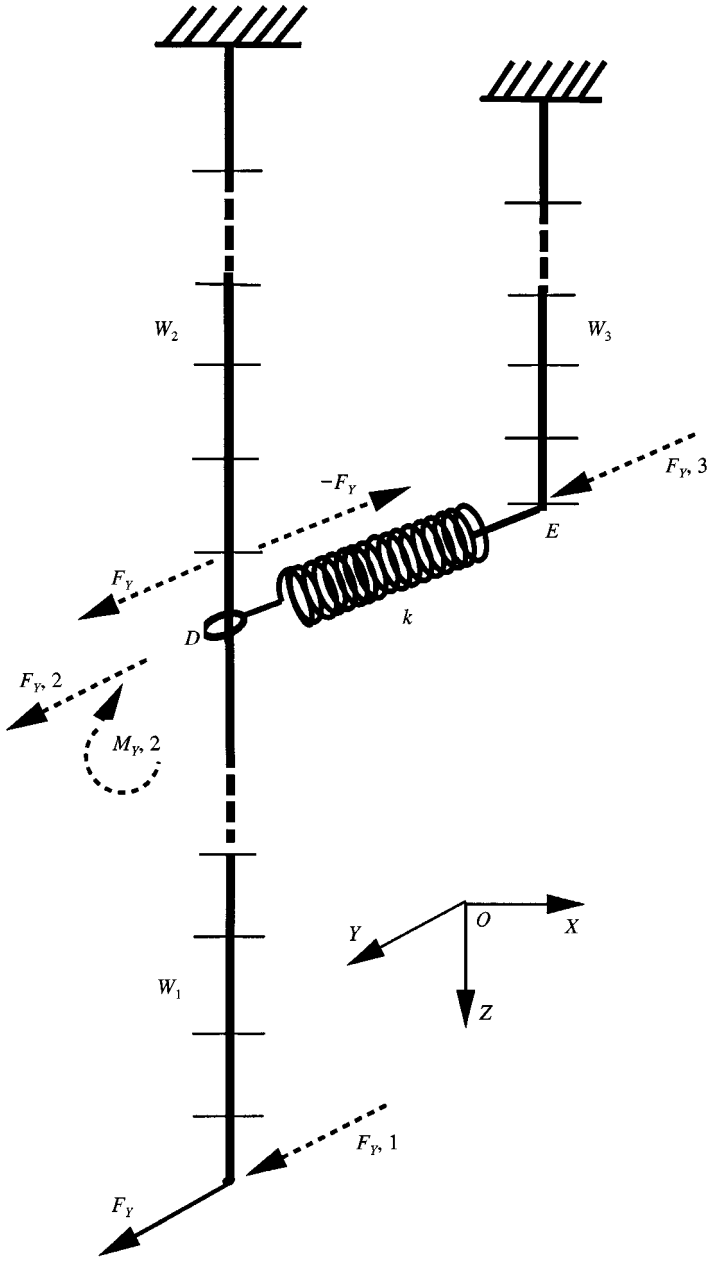

Figure 2. Line diagram of cantilever with intermediate support.

and all the local y-axes are coplanar and parallel to exciting force F_y. Hence, the x and y co-ordinates are the same for both the local and global sets of axes, while the z co-ordinate is different for local and global systems only in magnitude and origin position. Let $l_{m,i}$ be the length of the ith segment and $L_{m,i}$ be the distance of its origin from the bottom end of the lever, the point of application of the exciting

force F_x and F_y. Then,

$$\bar{L}_{m,i} = l_{m,1} + l_{m,2} + \cdots + l_{m,i} = \sum_{j=1}^{i} l_{m,j}. \tag{2}$$

The force F_y at the bottom end of the cantilever will induce forces $F_{y,m}$ and the pure bending moments $M'_{y,m}$ at the bottom end of the mth link. If the annular ring is flexible, only the force, $F_{y,3}$, will be transmitted to the link W_3 given by

$$F_{y,3} = k_S(Y_{2,1} - Y_{3,1}),$$

where k_S is the stiffness of the annular flexible ring and $Y_{2,1}$ and $Y_{3,1}$ are the end deflections of the two links denoted by W_2 and W_3 in Figure 2. This means that the pure bending moments induced at the end of links W_1 and W_3 are both zero. In general, however, the force and the bending moment will be shared by the two. Hence,

$$M'_{y,1} = 0.$$

At the point D on the link W_2, bending moment M'_y and a force F_y will be exerted due to the force F_y acting at the terminal end of the link W_1, where

$$M'_y = F_y\bar{L}_{1,n} = M'_{y,2} + M'_{y,3} = (c_2 + c_3)M'_y,$$

i.e.,

$$M'_{y,i} = c_i M'_y,$$

where $c_1 = 0$ and $c_2 + c_3 = 1$.

Also the force F_y will be shared by the link W_3 as given by the equation

$$F_y = F_{y,1} = F_{y,2} + F_{y,3} = (a_2 + a_3)F_y,$$

that is,

$$F_{y,m} = a_m F_y,$$

where $a_1 = 1$, $a_3 = F_y/F_{y,3}$ and $a_2 = 1 - a_3$.

Thus, from equation (1), the deflection $y_{m,i}$ of the ith segment of the mth link is given by the equation

$$y''_{m,i} = \frac{(\bar{L}_{m,i} - z_{m,i})F_{y,m} + M'_{y,m}}{E_{m,i}I_{m,i}}$$

or

$$y''_{m,i} = \frac{(\bar{L}_{m,i} - z_{m,i})a_m F_y + c_m M'_y}{E_{m,i}I_{m,i}}$$

which for $m = 1$, reduces to the equation given by

$$y''_{m,i} = \frac{(\bar{L}_{m,i} - z_{m,i})a_m F_y}{E_{m,i}I_{m,i}}$$

while for $m = 2$ or 3, the equation is

$$y''_{m,i} = \frac{(\bar{L}_{m,i} - z_{m,i})a_m F_y + c_m M'_y}{E_{m,i} I_{m,i}}$$

or

$$y''_{m,i} = \frac{(\bar{L}_{m,i} - z_{m,i})a_m F_y + c_m F_y \bar{L}_{1,n}}{E_{m,i} I_{m,i}}$$

$$= \frac{(\bar{L}_{m,i} + c_m \bar{L}_{1,n}/a_m - z_{m,i})a_m F_y}{E_{m,i} I_{m,i}}$$

Thus, in general, the lateral deflection of a cantilever link is given by

$$y''_{m,i} = \frac{(L_{m,i} - z_{m,i})a_m F_y}{E_{m,i} I_{m,i}} \tag{3}$$

where

$$L_{m,i} = \bar{L}_{m,i} + r_m \bar{L}_{1,n_1}.$$

Here $r_m = c_m/a_m$ with $c_1 = 0$ for $m = 1$. Similar expressions for deflection in the x direction will evolve with F_x in place of F_y and b_m in place of a_m.

3. MULTI-SEGMENT CANTILEVER DEFLECTION

From equation (3), the deflection in the y direction of a point P on the ith segment at distance $z_{m,i}$ from its local origin as shown in Figure 3 is given by

$$y''_{m,i} = (L_{m,i} - z_{m,i})\frac{F_{m,y}}{E_{m,i,x} I_{m,i,x}}$$

$$= (L_{m,i} - z_{m,i})\frac{a_m F_y}{E_{m,i,x} I_{m,i,x}}$$

$$= A_{m,i,y}(L_{m,i} - z_{m,i})a_m F_y \tag{4}$$

and in the x direction,

$$x''_{m,i} = (L_{m,i} - z_{m,i})\frac{F_{m,x}}{E_{m,i,y} I_{m,i,y}}$$

$$= (L_{m,i} - z_{m,i})\frac{b_m F_x}{E_{m,i,y} I_{m,i,y}}$$

$$= A_{m,i,x}(L_{m,i} - z_{m,i})b_m F_x, \tag{5}$$

where F_x and F_y are the end-exciting forces, $F_{m,x}$ and $F_{m,y}$ are the forces induced at the bottom end of the mth link and $z_{m,i}$ is the local co-ordinate of the point P under consideration. Here,

$$A_{m,i,y} = \frac{1}{E_{m,i,x} I_{m,i,x}}$$

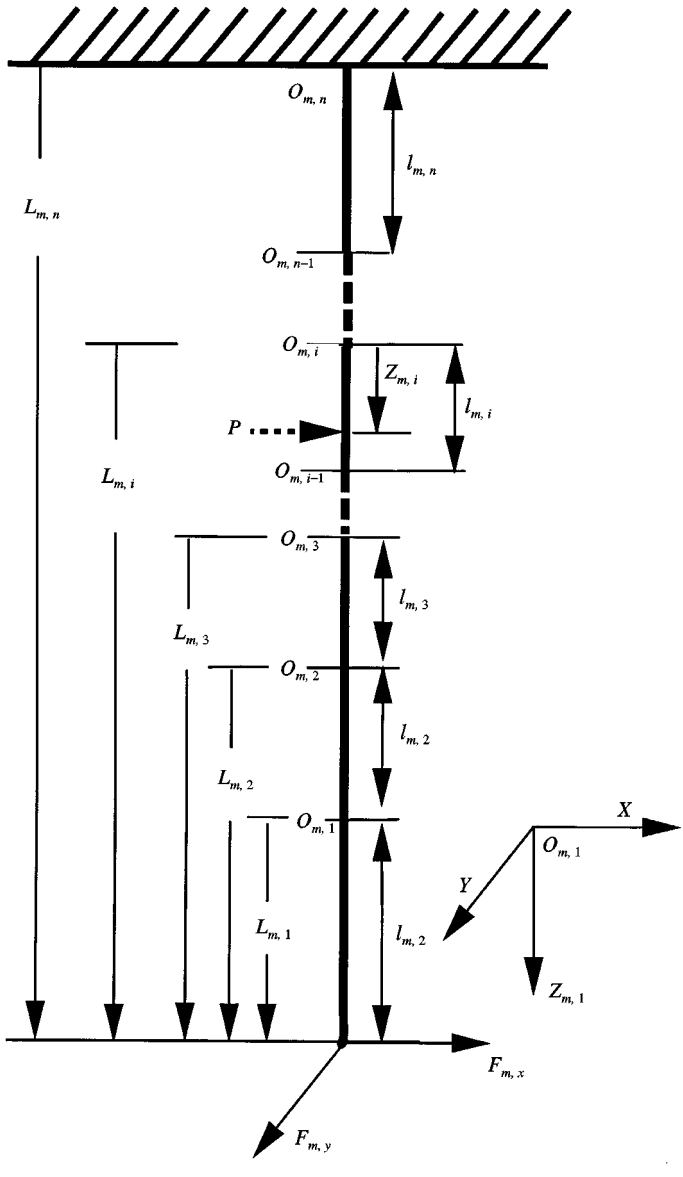

Figure 3. Segmented mth link of cantilever.

and

$$A_{m,x,y} = \frac{1}{E_{m,i,y} I_{m,i,y}}.$$

Dropping the subscripts x and y and considering only the y direction for the time being, the corresponding equations are

$$\begin{aligned} y''_{m,i} &= A_{m,i}(L_{m,i} - z_{m,i}) a_m F, \\ &= [A(L - z)]_{m,i}\, a_m F, \end{aligned} \tag{6}$$

integrating w.r.t. y

$$y'_{m,i} = \left[A\left(Lz - \frac{z^2}{2} + B \right) \right]_{m,i} a_m F,$$
$$= a_m F f_o(z, m, i) \quad \text{(say)} \tag{7}$$

and integrating once again w.r.t. y

$$y_{m,i} = \left[A\left(\frac{Lz^2}{2} - \frac{z^3}{6} + Bz + C \right) \right]_{m,i} a_m F,$$
$$= a_m F f_1(z, m, i). \tag{8}$$

The force divided integration constants $B_{m,i}$ and $C_{m,i}$ are evaluated from the condition that slope and displacement of the (m, i)th segment at $z_{m,i} = 0$ have the same values as those of the $(m, i+1)$th segment at $z_{m,i+1} = l_{m,i+1}$, i.e., at maximum z. Thus

$$B_{m,i} = \frac{Y'_{m,i+1}}{A_{m,i} a_m F},$$

$$C_{m,i} = \frac{Y_{m,i+1}}{A_{m,i} a_m F}.$$

Here

$$Y'_{m,i} = \max(y'_{m,i}) = \left[A\left(Ll - \frac{l^2}{2} + B \right) \right]_{m,i} a_m F = a_m F f_o(l, m, i),$$

$$Y_{m,i} = \max(y_{m,i}) = \left[A\left(\frac{Ll^2}{2} - \frac{l^3}{6} + Bl + C \right) \right]_{m,i} a_m F = a_m F f_1(l, m, i),$$

and the terminal end deflection $Y_{1,1}$ is given by

$$Y_{1,1} = \max(y_{1,1}) = \left[A\left(\frac{Ll^2}{2} - \frac{l^3}{6} + Bl + C \right) \right]_{1,1} a_1 F = a_1 F f_1(l, 1, 1)$$
$$= a_1 F/q = F/q,$$

where

$$q = \frac{1}{f_1(l, 1, 1)}.$$

The deflection, slope and other similar quantities along with their derivatives in terms of F render the model very complex, which is simplified by normalizing it with $Y_{1,1}$ to have all such quantities in terms of $Y_{1,1}$. Thus, the deflection of the (m, i)th segment at distance $z_{m,i}$ from the top of the segment in terms of overall terminal end deflection $Y_{1,1}$, with $a_1 = 1$, is given by

$$\frac{y_{m,i}}{Y_{1,1}} = \frac{a_m F f_1(z, m, i)}{F f_1(l, 1, 1)} = a_m q f_1(z, m, i)$$

or

$$y_{m,i} = Y_{1,1} a_m q f_1(z, m, i). \tag{9}$$

Also,

$$Y_{m,i} = Y_{1,1} a_m q f_1(l, m, i), \tag{10}$$

$$\dot{y}_{m,i} = \dot{Y}_{1,1} a_m q f_1(z, m, i), \tag{11}$$

$$\dot{Y}_{m,i} = \dot{Y}_{1,1} a_m q f_1(l, m, i), \tag{12}$$

$$y'_{m,i} = Y_{1,1} a_m q f_o(z, m, i), \tag{13}$$

$$Y'_{m,i} = Y_{1,1} a_m q f_o(l, m, i). \tag{14}$$

With the above simplification,

$$B_{m,i} = \frac{Y'_{m,i+1}}{qY_{1,1} a_m A_{m,i}} = \frac{qY_{1,1} a_m f_o(l, m, i+1)}{qY_{1,1} a_m A_{m,i}} = \frac{f_o(l, m, i+1)}{A_{m,i}},$$

$$C_{m,i} = \frac{Y_{m,i+1}}{qY_{1,1} a_m A_{m,i}} = \frac{qY_{1,1} a_m f_1(l, m, i+1)}{qY_{1,1} a_m A_{m,i}} = \frac{f_1(l, m, i+1)}{A_{m,i}},$$

while

$$B_{2,n} = B_{3,n} = C_{2,n} = C_{3,n} = 0$$

and

$$B_{1,n} = \frac{Y'_{2,1}}{qY_{1,1} A_{1,n} a_1} = \frac{qY_{1,1} a_2 f_o(l, 2, 1)}{qY_{1,1} a_1 A_{1,n}} = \frac{a_2 f_o(l, 2, 1)}{A_{1,n}},$$

$$C_{1,n} = \frac{Y_{2,1}}{qY_{1,1} A_{1,n} a_1} = \frac{qY_{1,1} a_2 f_1(l, 2, 1)}{qY_{1,1} a_1 A_{1,n}} = \frac{a_2 f_1(l, 2, 1)}{A_{1,n}},$$

since $a_1 = 1$.

4. ENERGY EQUATION OF THE SYSTEM

According to energy conservation for an undamped system, the sum of kinetic and potential energies is constant. Simplification of the equation thus arrived at by summing up the component potential and kinetic energies of the system at any time will give the equation of motion of the undamped free vibrating system. The kinetic and potential energies are evaluated as follows.

4.1. KINETIC ENERGY OF THE SYSTEM

The kinetic energy of the system is given by

$$KE = KE_M + KE_T \tag{15}$$

where (KE_M) is the kinetic energy of the suspended masses and (KE_T) is that of all the segments in all the links.

4.1.1. *Kinetic energy of the suspended masses*

With the help of equation (12), the kinetic energy ($KE_{M_{m,i}}$) of the mass $M_{m,i}$ suspended at the lower end of the (m, i)th segment is given by

$$KE_{M_{m,i}} = \frac{M_{m,i}\dot{Y}_{m,i}^2}{2} = \frac{M_{m,i}q^2\dot{Y}_{1,1}^2}{2}[f_1(l,m,i)]^2 a_m^2 = \frac{M_{m,i}q^2\dot{Y}_{1,1}^2}{2} f_2(l,m,i)a_m^2,$$

and the KE_M of all the suspended masses is given by

$$KE_M \frac{q^2\dot{Y}_{1,1}^2}{2} \sum_{m=1}^{3} a_m^2 \sum_{i=1}^{n} M_{m,i} f_2(l,m,i). \tag{16}$$

Here $M_{m,i}$ will be zero for the segment with no suspended mass.

4.1.2. *Kinetic energy of the segment mass*

The kinetic energy KE_T of the total n segments of all the links with the help of equation (11) is given by

$$\begin{aligned} KE_T &= \frac{1}{2}\sum_{m=1}^{3} a_m^2 \sum_{i=1}^{n} \int_0^{l_{m,i}} m_{m,i}\dot{y}_{m,i}^2 \,\mathrm{d}z \\ &= \frac{1}{2}\sum_{m=1}^{3} a_m^2 \sum_{i=1}^{n} m_{m,i} \int_0^{l_{m,i}} \dot{Y}_{1,1}^2 q^2 [f_1(z,m,i)]^2 \,\mathrm{d}z \\ &= \frac{1}{2}\sum_{m=1}^{3} a_m^2 \sum_{i=1}^{n} m_{m,i}\, \dot{Y}_{1,1}^2 q^2 \int_0^{l_{m,i}} [f_1(z,m,i)]^2 \,\mathrm{d}z \\ &= \frac{\dot{Y}_{1,1}^2 q^2}{2} \sum_{m=1}^{3} a_m^2 \sum_{i=1}^{n} m_{m,i} f_3(l,m,i). \end{aligned} \tag{17}$$

Here $m_{m,i}$ is the mass per unit length of the ith segment of the mth link and

$$\begin{aligned} f_3(l,m,i) &= \int_0^{l_{m,i}} [f_1(z,m,i)]^2 \,\mathrm{d}z \\ &= \int_0^{l_{m,i}} \left[A\left\{\left(\frac{Lz^2}{2} - \frac{z^3}{6}\right) + Bz + C\right\}\right]_{m,i}^2 \mathrm{d}z \end{aligned}$$

$$= \int_0^{l_{m,i}} \left[A^2 \left\{ \left(\frac{L^2 z^4}{4} + \frac{z^6}{36} - \frac{L z^5}{6} \right) + B^2 z^2 + C^2 + B \left(L z^3 - \frac{z^4}{3} \right) + 2BCz + C \left(L z^2 - \frac{z^3}{3} \right) \right\} \right]_{m,i} \mathrm{d}z$$

$$= \left[A^2 \left\{ \left(\frac{L^2 l^5}{20} + \frac{l^7}{252} - \frac{L l^6}{36} \right) + \frac{B^2 l^3}{3} + C^2 l + B \left(\frac{L l^4}{4} - \frac{l^5}{15} \right) + C \left(\frac{L l^3}{3} - \frac{l^4}{12} \right) + BC l^2 \right\} \right]_{m,i}.$$

Thus, from equations (15)–(17), the KE of the whole system is given by

$$KE = \left[\sum_{m=1}^{3} a_m^2 \sum_{i=1}^{n} \{ M_{m,i} f_2(l, m, i) + m_{m,i} f_3(l, m, i) \} \right] \frac{q^2 \dot{Y}_{1,1}^2}{2}. \tag{18}$$

4.2. POTENTIAL ENERGY OF THE SYSTEM

The potential energy PE of the system is the sum of PE_E, the potential energy stored against stiffness of all cantilever segments, PE_T, potential energy due to gain in height of the weight of all segments and PE_M, potential energy due to rise in the suspended masses against gravity. Thus, the total potential energy PE is given by

$$PE = PE_E + PE_T + PE_M. \tag{19}$$

The individual potential energies are formulated in the following subsections.

4.2.1. *Elastic stiffness energy*

The potential energy stored in the hanging cantilever due to its material stiffness is given by

$$PE_E = \int_0^{Y_{1,1}} F \, \mathrm{d}Y_{1,1}.$$

Since $F = qY_{1,1}$,

$$PE_E = \int_0^{Y_{1,1}} qY_{1,1} \, \mathrm{d}Y_{1,1} = \frac{qY_{1,1}^2}{2}. \tag{20}$$

4.2.2. *Rise of an element against gravity*

As shown in Figure 4, the rise of an element $\mathrm{d}s$ at a distance z from the top of the segment against gravity during bending is given by

$$h = \int \mathrm{d}h = \int_0^z (\mathrm{d}s - \mathrm{d}w) = \int_0^z (\mathrm{d}s - \sqrt{\mathrm{d}s^2 - \mathrm{d}y^2})$$

$$= \int_0^z [1 - \{1 - (y')^2\}^{1/2}] \, \mathrm{d}s = \int_0^z [1 - \{1 - \tfrac{1}{2}(y')^2\}] \, \mathrm{d}s = \frac{1}{2} \int_0^z (y')^2 \, \mathrm{d}s$$

since $y' \ll 1$.

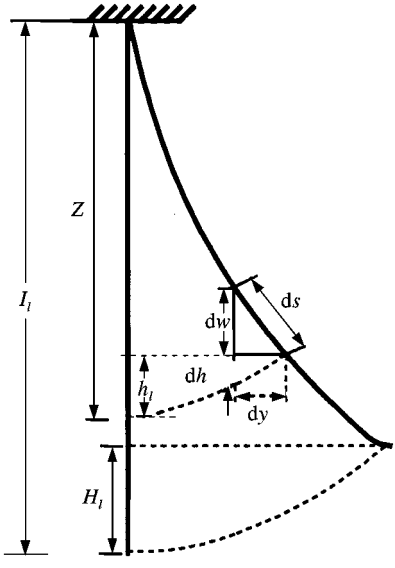

Figure 4. Segment deflection.

Following the analysis of section 3 (equation (7)), the rise of the ith segment is given by

$$h_{m,i} = \frac{1}{2}\int_0^{z_{m,i}} (y'_{m,i})^2 \, \mathrm{d}s$$

$$= \frac{1}{2}\int_0^{z_{m,i}} a_m^2 \left[A\left(Ls - \frac{s^2}{2} + B \right) \right]_{m,i}^2 \mathrm{F}^2 \, \mathrm{d}s$$

$$= \frac{Y_{1,1}^2 q^2 a_m^2}{2} \left[A^2 \left\{ \left(\frac{L^2 z^3}{3} + \frac{z^5}{20} - \frac{Lz^4}{4} \right) + B\left(Lz^2 - \frac{z^3}{3} \right) + B^2 z \right\} \right]_{m,i}$$

$$= \frac{Y_{1,1}^2 q^2 a_m^2}{2} f_4(z, m, i),$$

and its maximum value is given by

$$H_{m,i} = \frac{Y_{1,1}^2 q^2 a_m^2}{2} f_4(l, m, i).$$

The overall or global rise of an element is given by

$$u_{m,i} = h_{m,i} + \sum_{j=i+1}^{n} H_{m,j}. \tag{21}$$

The overall or global rise of a segment bottom end is given by

$$U_{m,i} = \sum_{j=i}^{n} H_{m,j}. \tag{22}$$

4.2.3. *Potential energy of the suspended masses*

Using equation (22), the potential energy of a suspended mass $M_{m,i}$ is given by

$$PE_{M_{m,i}} = M_{m,i}\, g U_{m,i} = M_{m,i}\, g \sum_{j=i}^{n} H_{m,j}$$

$$= \frac{M_{m,i}\, g Y_{1,1}^2 q^2 a_m^2}{2} \sum_{j=i}^{n} f_4(l, m, j),$$

and the potential energy of all the suspended masses of all the links is given by

$$PE_M = \sum_{m=1}^{3} a_m^2 \sum_{i=1}^{n} M_{m,i}\, g U_{m,i} = \frac{g Y_{1,1}^2 q^2}{2} \sum_{m=1}^{3} a_m^2 \sum_{i=1}^{n} \left[M_{m,i} \sum_{j=i}^{n} f_4(l, m, j) \right]. \tag{23}$$

4.2.4. *Potential energy due to segments' weight*

Using equation (21), the potential energy of a small element of the (m, i)th segment due to its weight is given by

$$\mathrm{d}(PE_T)_{m,i} = m_{m,i} g u_{m,i}\, \mathrm{d}z,$$

where $m_{m,i}$ is mass per unit length of the (m, i)th segment of the cantilever. Thus

$$(PE_T)_{m,i} = m_{m,i} g \int_0^{l_{m,i}} u_{m,i}\, \mathrm{d}z = m_{m,i} g \int_0^{l_{m,i}} \left(h_{m,i} + \sum_{j=i+1}^{n} H_{m,j} \right) \mathrm{d}z$$

$$= \frac{m_{m,i} g Y_{1,1}^2 q^2 a_m^2}{2}$$

$$\times \left[\left\{ A^2 \left(\frac{L^2 l^4}{12} + \frac{l^6}{120} - \frac{L l^5}{20} + \frac{B^2 l^2}{2} + B \left(\frac{L l^3}{3} - \frac{l^4}{12} \right) \right) \right\}_{m,i} + l \sum_{j=i+1}^{n} f_4(l, m, j) \right]$$

$$= \frac{m_{m,i} g Y_{1,1}^2 q^2 a_m^2}{2} \left[f_6(l, m, i) + l_{m,i} \sum_{j=i+1}^{n} f_4(l, m, j) \right] = \frac{m_{m,i} g Y_{1,1}^2 q^2 a_m^2}{2} f_5(l, m, i).$$

The PE_T for all segments of all the links is given by

$$PE_T = \sum_{m=1}^{3} a_m^2 \sum_{i=1}^{n} (PE_T)_{m,i} = \frac{Y_{1,1}^2 q^2 g}{2} \sum_{m=1}^{3} a_m^2 \sum_{i=1}^{n} m_{m,i} f_5(l, m, i). \tag{24}$$

Thus, by summing up its component given by equations (19), (20), (23) and (24), the total PE of the system is

$$PE = \frac{q Y_{1,1}^2}{2} + \frac{g Y_{1,1}^2 q^2}{2} \sum_{m=1}^{3} a_m^2 \sum_{i=1}^{n} \left[M_{m,i} \sum_{j=i}^{n} f_4(l, m, j) + m_{m,i} f_5(l, m, i) \right]. \tag{25}$$

5. EQUATION OF MOTION OF AN UNDAMPED FREE SYSTEM

The energy conservation equation of the system is

$$KE + PE = constant.$$

With the values of KE and PE given by equations (18) and (25), the above equation becomes

$$\left[q_y^2 \sum_{m=1}^{3} a_m^2 \sum_{i=1}^{n} \{M_{m,i} f_2(l, m, i) + m_{m,i} f_3(l, m, i)\}\right] \frac{\dot{Y}_{1,1}^2}{2}$$
$$+ \left[q_y + g q_y^2 \sum_{m=1}^{3} a_m^2 \sum_{i=1}^{n} \left\{M_{m,i} \sum_{j=i}^{n} f_4(l, m, j) + m_{m,i} f_5(l, m, i)\right\}\right] \frac{\dot{Y}_{1,1}^2}{2} = constant.$$

By differentiating with respect to time, simplifying, rewriting the subscript y and replacing Y_1 simply by Y, the equation becomes

$$M_y \ddot{Y} + K_y Y = 0. \tag{26}$$

Similarly for deflection in the x direction, the equation is

$$M_x \ddot{X} + K_x X = 0, \tag{27}$$

where

$$M_y = \left[q_y^2 \sum_{m=1}^{3} a_m^2 \sum_{i=1}^{n} \{M_{m,i} f_2(l, m, i) + m_{m,i} f_3(l, m, i)\}\right]_y, \tag{28}$$

$$M_x = \left[q_x^2 \sum_{m=1}^{3} b_m^2 \sum_{i=1}^{n} \{M_{m,i} f_2(l, m, i) + m_{m,i} f_3(l, m, i)\}\right]_x, \tag{29}$$

$$K_y = \left[q_y + g q_y^2 \sum_{m=1}^{3} a_m^2 \sum_{i=1}^{n} \left\{M_{m,i} \sum_{j=i}^{n} f_4(l, m, j) + m_{m,i} f_5(l, m, i)\right\}\right]_y \tag{30}$$

and

$$K_x = \left[q_x + g q_x^2 \sum_{m=1}^{3} b_m^2 \sum_{i=1}^{n} \left\{M_{m,i} \sum_{j=i}^{n} f_4(l, m, j) + m_{m,i} f_5(l, m, i)\right\}\right]_x. \tag{31}$$

6. STRUCTURAL OR HYSTERESIS DAMPING

When the structural material is cyclically stressed, the energy is dissipated due to hysteresis losses, which are almost 0·2 times those of the strain energy of the system for most of the structural materials [13–15]. The strain energy of the system in Y directional vibrations (equation (20)) is given by

$$U_s = \frac{q_y Y^2}{2} \tag{32}$$

and equivalent damping energy dissipated per cycle [13, 14] is given by

$$U_d = \pi c_{ey} \omega Y^2,$$

where ω is the circular frequency of the vibration. With dissipation factor γ (0·2 for most of the metals), the relation becomes

$$\pi c_{ey} \omega Y^2 = \frac{\gamma q_y Y^2}{2}$$

or equivalent viscous damping is

$$c_{ey} = \frac{\gamma q_y}{2\pi\omega}. \tag{33}$$

The equivalent viscous damping force is thus

$$F_{dy} = \frac{\gamma q_y}{2\pi\omega} \dot{Y}.$$

Similarly for the X direction,

$$c_{ex} = \frac{\gamma q_x}{2\pi\omega} \tag{34}$$

and

$$F_{dx} = \frac{\gamma q_x}{2\pi\omega} \dot{X}.$$

7. EQUATION OF DAMPED FORCED VIBRATIONS

If F_x and F_y are two orthogonal exciting forces in the X and Y directions acting at the tip of the cantilever, then equations of damped forced vibrations are given by

$$M_y \ddot{Y} + C_{ey} \dot{Y} + K_y Y = F_y, \tag{35}$$

$$M_x \ddot{X} + C_{ex} \dot{X} + K_x X = F_x. \tag{36}$$

Viscous damping of the system is ignored to view the response of the model and its parameters exclusively. These are the second order differential equations of a forced vibrating system [13] with an equivalent viscous damping term resulting from cyclic hysteresis losses of structural strain energy.

8. SYSTEM MODEL, DATA AND SIMULATION

From the preceding sections, the mathematical model of the forced damped system is therefore given by

$$M_y \ddot{Y} = F_y - C_{ey} \dot{Y} - K_y Y, \tag{37}$$

$$M_x \ddot{X} = F_x - C_{ex} \dot{X} - K_x X, \tag{38}$$

where F_y and F_x are the exciting forces. Following the iterative computational technique for the initial value problems of special second order differential

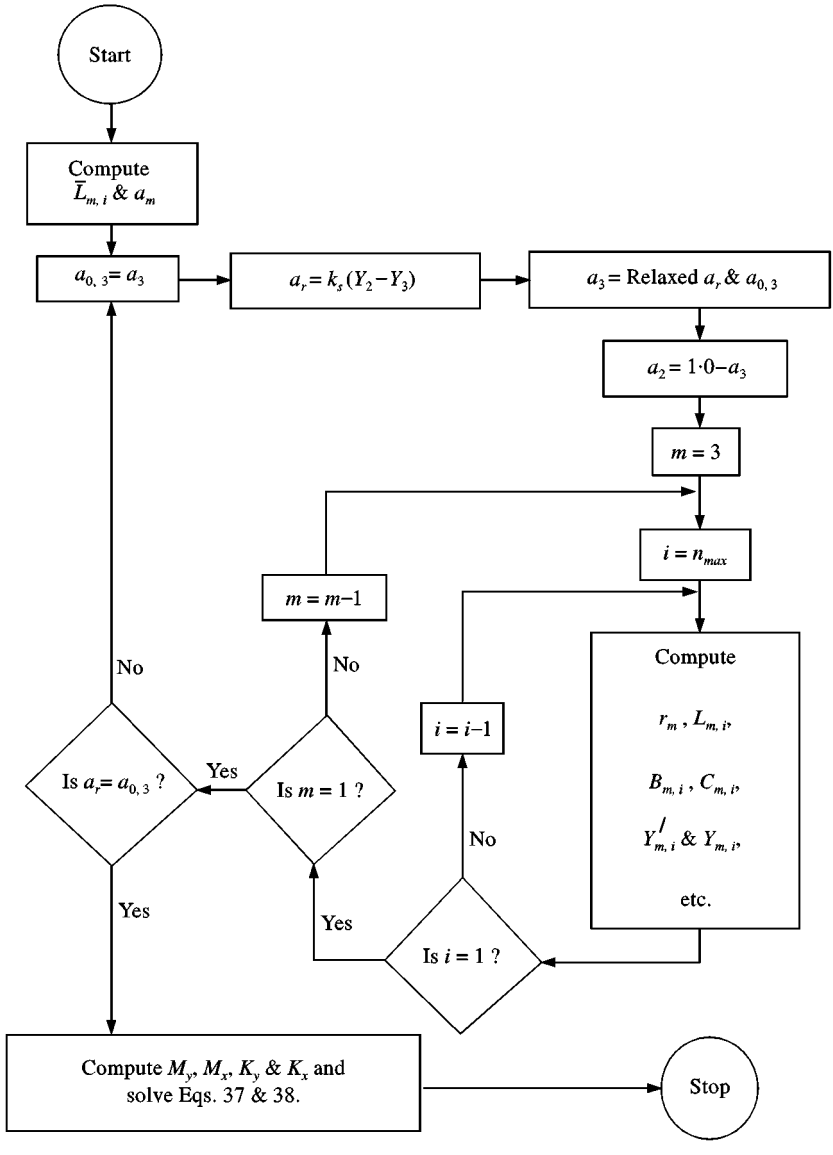

Figure 5. Block diagram for solution procedure.

equations [16], the computational model is developed for the system under consideration. Automatic halving of the time-step in case of non-convergence and intelligently doubling it after a few time-steps to get a faster solution with corresponding change of related terms in two cases have been added to the original scheme. The physical data of the system in the present case will need a computer code based on numerical methods, like the improved relaxation method [17], to converge the system with some implicit parameters introducing loop in this procedure as shown in block diagram in Figure 5. For instance, in this procedure, $Y_{2,1}$ and $Y_{3,1}$, the bottom end deflections of link numbers 2 and 3, depend upon

a_2 and a_3, the load-sharing ratios, respectively, while a_3 and hence a_2 depend upon $Y_{2,1}$ and $Y_{3,1}$. The mathematical model of the system is given by equations (37) and (38) and its response depends upon their coefficients given by expressions (28)–(34). As the summations in expressions (28)–(31) are over the links from 1 to 3 and a_3 and b_3 being non-zero, it is clear that the support tube has a definite and important role. The frequent presence of quantities pertaining to link no. 3, especially in the outer loop of the flow chart (Figure 5) also indicates the specific role of the support tube, but the positive or negative contribution of its parameters, however, cannot be directly assessed. Taking the cantilever and the support tube symmetric about the axis of the tube, only equation (37) may be solved to simulate the response of the system. The system simulated with the model developed and analyzed in this study comprises a 105 cm long inner aluminum tube, supporting a mass of 13 g at its bottom end and having 527 mm^4 moment of inertia concentric with a 2·0 mm thick aluminum support tube of various lengths and diameters (Figure 1). The damping response of the system in free vibration for a set of data is shown in Figure 6. This, however, does not elaborate the contribution of support tube parameters. To show their contribution, the analytical solution [13, 14, 18] of equation (37) is used both in free and forced vibrations. The geometric data of an experimental set-up was used to see the response of various parameters and results obtained are plotted in Figures 7–9. The effective mass M_y (equation (28)), effective spring constant K_y (equation (30)), the circular frequency ω_n given by

$$\omega_n = \sqrt{\frac{K_y}{M_y}}, \tag{39}$$

and the critical damping C_c given by

$$C_c = 2M_y\omega_n \tag{40}$$

are normalized by their respective values for minimum parametric values of the support tube and plotted together to see their response versus support tube parameters and also to compare their mutual behavior. Similar quantities pertaining to and characteristic of free and forced vibrations which may enable the comparison and show the control and damping response of support tube parameters are listed and defined in the following subsections and their normalized values are plotted in Figures 7–9.

8.1. FREE VIBRATIONS

The analytical solution of equation (37) for free vibration (i.e., with $F_y = 0$) is given by

$$y_f = Y_f e^{-\xi_f \omega_n t} \sin(\omega_d t + \phi_f) = \frac{Y_f}{E_f^t} \sin(\omega_d t + \phi_f)$$

or

$$y_f = A_f \sin(\omega_d t + \phi_f), \tag{41}$$

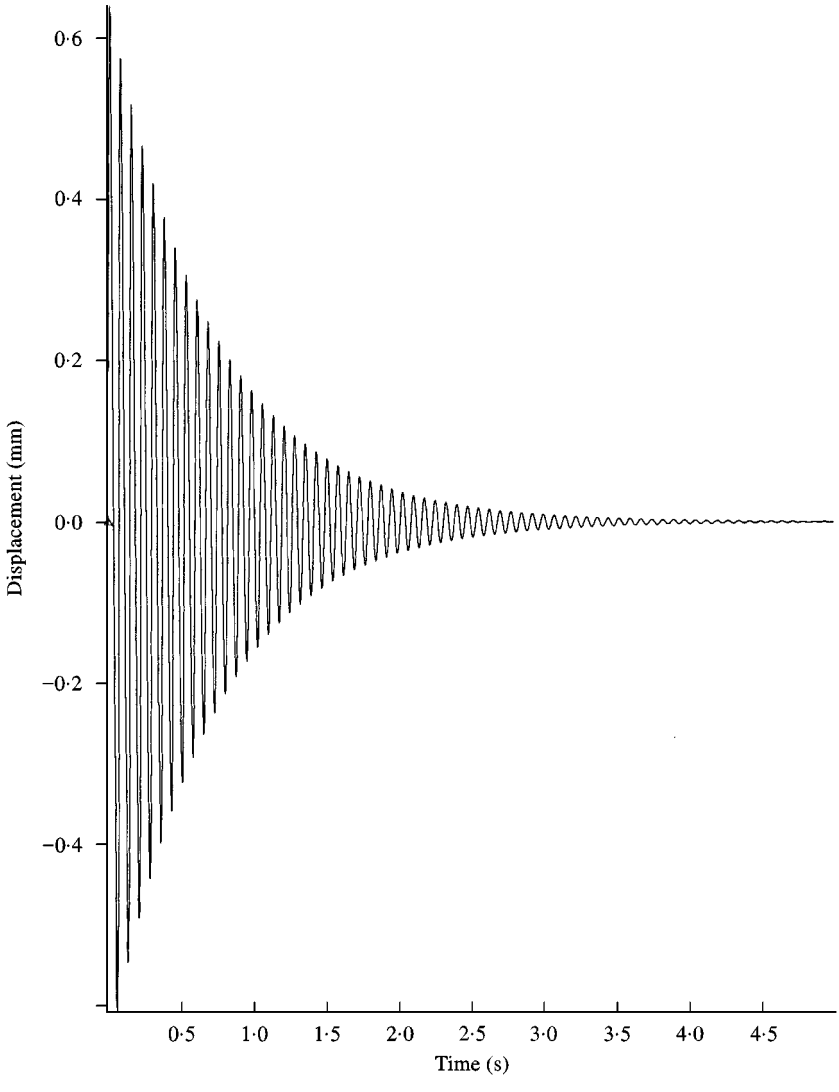

Figure 6. Time response of the system.

where ω_d, the frequency of damped oscillations is

$$\omega_d = \omega_n\sqrt{1-\xi_f^2}, \tag{42}$$

ϕ_f, the phase angle in free vibration with zero initial velocity is

$$\phi_f = \tan^{-1}\left(\frac{\sqrt{1-\xi_f^2}}{\xi_f}\right), \tag{43}$$

Y_f, the initial maximum deflection under constant initial potential energy input U_s, (equation (32)) is

$$Y_f = \sqrt{\frac{2U_s}{q_y}}, \tag{44}$$

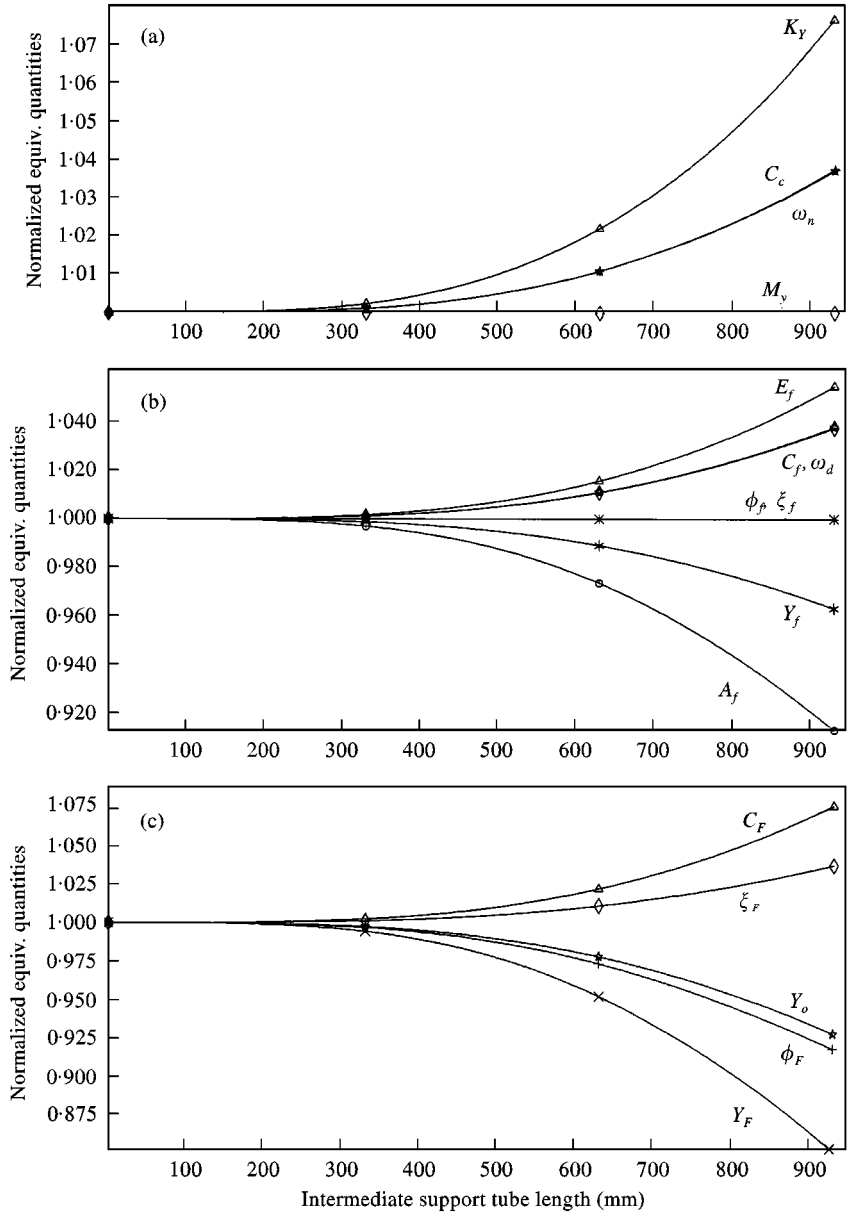

Figure 7. Response versus support tube length of (a) system constants, (b) free vibration parameters, (c) forced vibration parameters.

ξ_f, the damping factor is

$$\xi_f = \sqrt{\frac{C_f}{C_c}}, \tag{45}$$

and the base value of vibration amplitude reduction term is

$$E_f = e^{\xi_f \omega_n}, \tag{46}$$

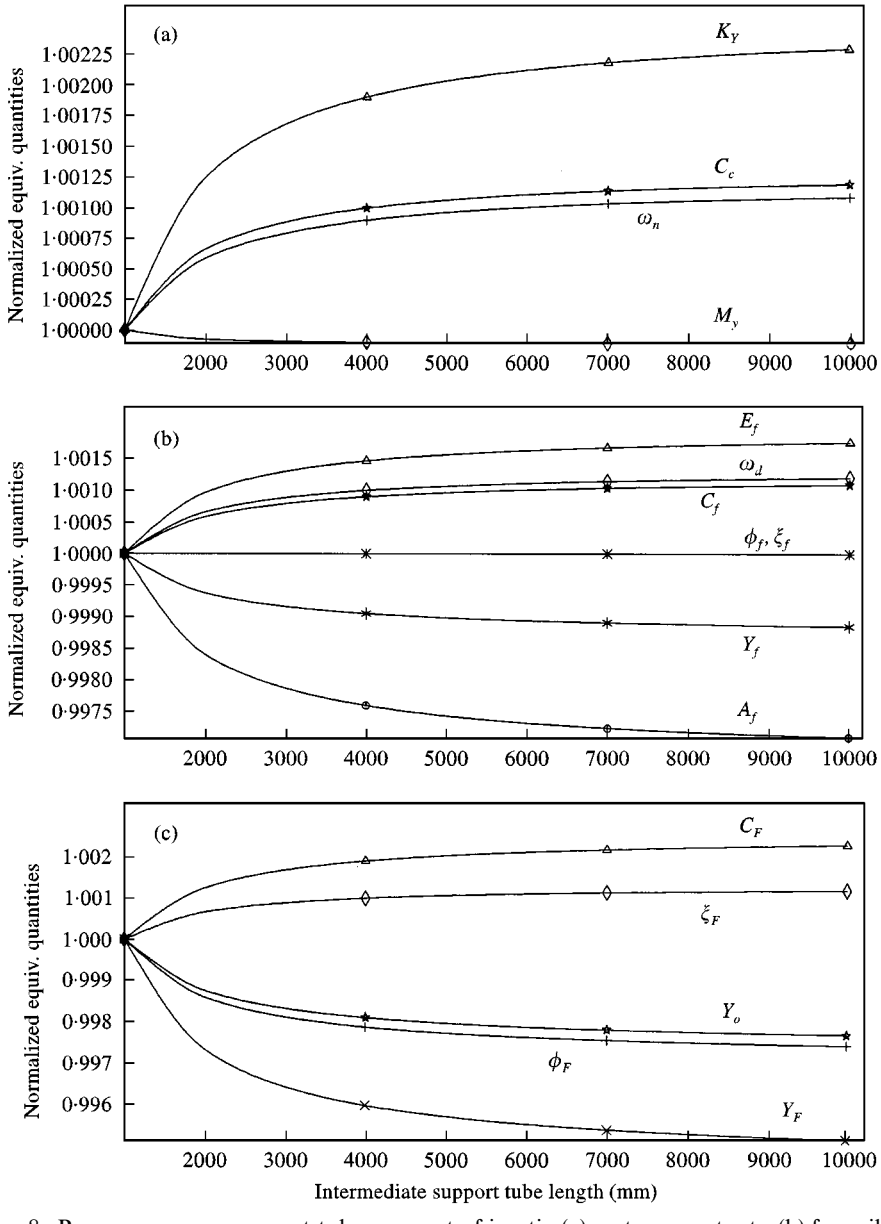

Figure 8. Response versus support tube moment of inertia (a) system constants, (b) free vibration parameters, (c) forced vibration parameters.

and the net unit time vibration amplitude is given by

$$A_f = \frac{Y_f}{E_f}. \tag{47}$$

Here C_f is the damping coefficient in free vibrations given by equation (33) with $\omega = \omega_n$ and C_c given by equation (40).

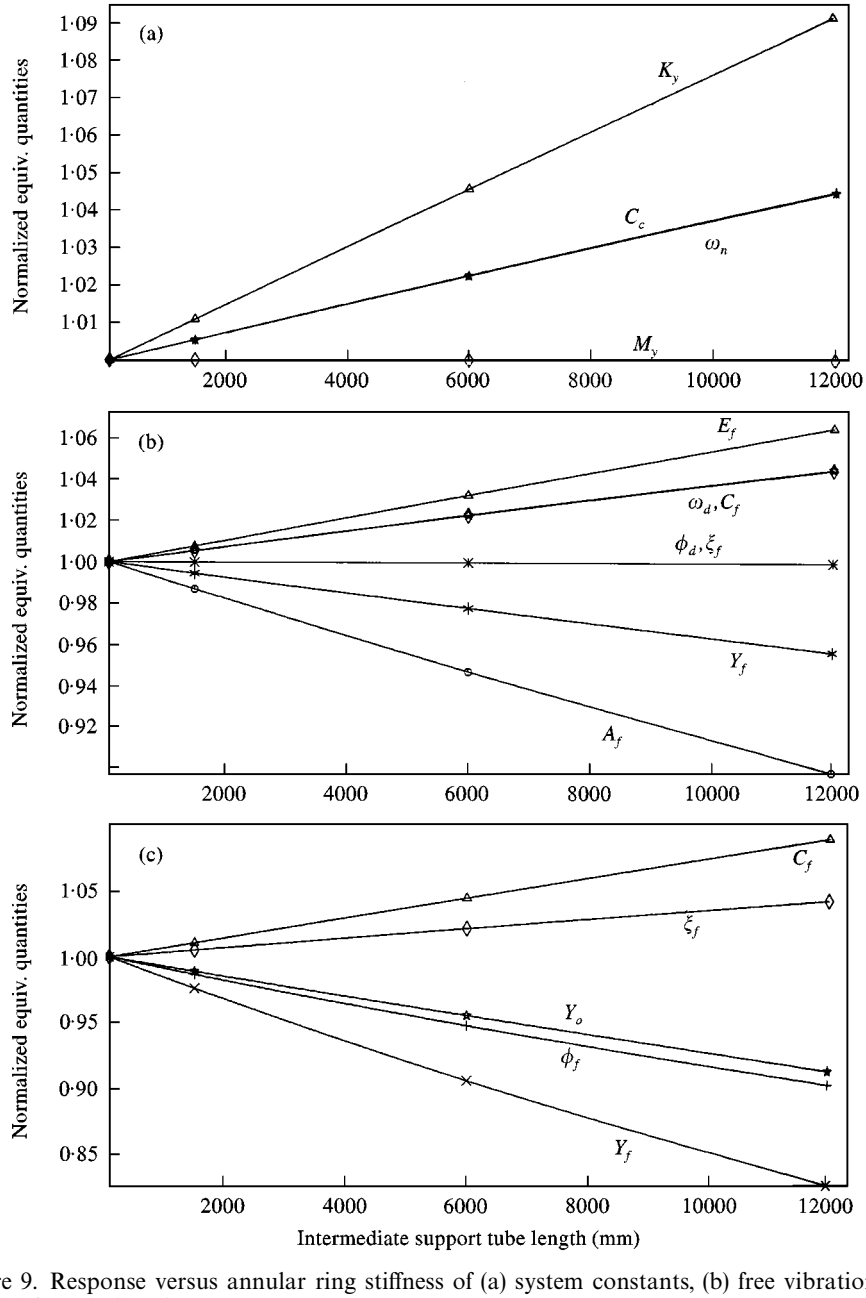

Figure 9. Response versus annular ring stiffness of (a) system constants, (b) free vibration parameters, (c) forced vibration parameters.

8.2. FORCED VIBRATIONS

The steady state analytical solution of equation (37) for forced vibration is given by

$$y_F = Y_F \sin(\omega t - \phi_F), \tag{48}$$

where ω is the circular frequency of exciting force, while ϕ_F, the phase angle, is given by

$$\phi_F = \tan^{-1}\left(\frac{2\xi_F(\omega/\omega_n)}{1-(\omega/\omega_n)^2}\right), \tag{49}$$

Y_F, the amplitude of deflection in forced vibration, is given by

$$Y_F = \frac{Y_0}{\sqrt{[1-(\omega/\omega_n)^2]^2 + [2\xi_F(\omega/\omega_n)]^2}}, \tag{50}$$

ξ_F, the damping factor in forced vibrations, is given by

$$\xi_F = \sqrt{\frac{C_F}{C_c}}, \tag{51}$$

and Y_0, the zero frequency deflection, is given by

$$Y_0 = \frac{F_0}{K_y}. \tag{52}$$

Here C_F is the damping coefficient in forced vibrations given by equation (33) with ω being the frequency of the exciting force.

9. RESULTS' ANALYSIS AND DISCUSSIONS

Figure 6 shows the overall damping response of the system. The positive or negative contribution of the support tube parameters cannot be assessed from this figure. Figures 7–9, however, show the response of three main support tube parameters, viz., tube length, moment of inertia and annular ring stiffness respectively. Part (a) of these figures show the response of the system's overall constants versus support tube parameters, part (b) shows the vibration characteristics in case of free vibrations of the system under the same exciting energy input and part (c) shows the vibration characteristics in case of forced vibrations of the system under the same continuous harmonic excitation. The response of these parameters is elaborated in the following sections.

9.1. SUPPORT TUBE RESPONSE

The response of the two parameters of the support tube is discussed in the following subsections.

9.1.1. *Length response*

Figure 7 shows that the system constants, namely the effective spring constant K_y, the critical damping coefficient C_c and the natural frequency ω_n, increase non-linearly with the length while the effective mass M_y remains almost constant. The rise in K_y, C_c and ω_n, however, is insignificant in the region within 500 mm length of the support tube, while beyond this they increase exponentially with

length. In case of free vibrations, the time-based reduction term E_f, damping coefficient C_f and damped frequency ω_d increase while both initial amplitude of vibration Y_f and its net value at unit time A_f decrease with the tube length. The phase angle ϕ_f and the damping ratio ξ_f do not change appreciably. From this it is evident that increase in support tube length contributes positively. Within 500 mm support tube length, its contribution is insignificant, while beyond this its effectiveness increases exponentially. In the case of forced vibrations both damping coefficient C_F and damping ration ξ_F increase while initial amplitude Y_0, phase angle ϕ_F and net amplitude Y_F decrease with length. This shows that the support tube length contributes positively to damping as well as control of forced vibrations. The contribution of the support tube length has two aspects, viz. resistance to the initial amplitude throw and quicker damping of the excited vibrations. Both of these positive aspects increase with the length of the support tube, though they are insignificant in earlier regions.

It is also clear from the results (Figure 7) that in the present set-up 300 mm length of support tube is almost ineffective. However, beyond this it becomes effective particularly above the length of 700 mm; its contribution is quite reasonable. This provides an adjustable parameter to suitably control the possible vibration problem.

9.1.2. *Moment of innertia response*

Figure 8 shows that the system constants, viz., the effective spring constant K_y, the critical damping C_c and natural frequency ω_n, increase non-linearly with the moment of inertia of the support tube while the effective mass M_y remains almost constant with slight initial decrease. This contribution, however, is significant in the region within 3000 mm^4 of moment of inertia of the support tube, while beyond this the behavior is asymptotic. In the case of free vibrations, the time-based reduction term E_f, damping coefficient C_f and damped frequency ω_d again increase, while both initial amplitude of vibration and its net value at unit time A_f decrease asymptotically with the increase in moment of inertia of the support tube. The phase angle ϕ_f and the damping ratio ξ_f again do not change appreciably. From this it is evident that the increase in moment of inertia of support tube contributes positively. However, in the region beyond 3000 mm^4 its contribution diminishes asymptotically. In the case of forced vibrations, both the damping coefficient and damping ratio ξ_F increase while initial amplitude Y_0, phase angle ϕ_F and net amplitude Y_F decrease with the increase in moment of inertia of the support tube. This shows that the support tube moment of inertia contributes positively to damping as well as control of forced vibrations. The contribution of the support tube moment of inertia has again two aspects, viz., resistance to the initial amplitude throw and quicker damping of the excited vibrations. Both these positive aspects increase with the moment of inertia of the support tube, though they become less significant beyond 3000 mm^4. The suitable values of second moment of area for the system under consideration is thus below 3000 mm^4. Beyond this the further gain in control of oscillation amplitude and damping of perturbation is very small. The former zone is most suitable as its effectiveness increases sharply and the

later becomes ineffective because of its slight further gain. This provides another adjustable parameter to suitably handle the possible vibrations.

9.2. ANNULAR RING RESPONSE

Figure 9 shows that the system constants, namely the effective spring constant K_y, the critical damping C_c and natural frequency ω_n increase linearly with the annular ring stiffness, while the effective mass M_y remains constant. In the case of free vibrations, the time-based reduction term E_f, damping coefficient C_f and damped frequency ω_d, increase while both initial amplitude of vibration Y_f and its net value at unit time A_f decrease with the annular ring stiffness. The phase angle ϕ_f and the damping ratio ξ_f do not change appreciably. This shows that increase in annular ring stiffness also contributes positively. In the case of forced vibrations, both damping coefficient C_F and damping ratio ξ_F increase, while initial amplitude Y_0, phase angle ϕ_F and net amplitude Y_F decrease with annular ring stiffness. This shows that the annular ring stiffness contributes positively to damping as well as control of the forced vibrations. The contribution of the annular ring stiffness also has two aspects, viz., resistance to the initial amplitude throw and quicker damping of the excited vibrations. Both these positive factors increase linearly with increase in the annular ring stiffness providing another suitable adjustable parameter to minimize the adverse effects of the possible perturbations.

9.3. MODAL RESPONSE OF THE PARAMETERS

Vibration amplitude was the critical parameter in the system under study in which the fundamental mode is a dominant one. In the higher mode shapes of vibrations, the amplitude of the bottom end of the inner tube will decrease further and in some of the mode shapes, the support point of the annular ring will become the node and hence the anti-node at the bottom end of the tube will decrease further depending upon its distance from the node. This will change the magnitudes of the response of the support tube parameters with no change in their trend.

A clear picture of the behavior of the support tube parameters is given above. The model developed can identify the optimal values of these parameters for a given set-up which can help to facilitate an overall better and safer system operation. Moreover, by appropriately setting the support tube length and second moment of the area to a certain suitable limit and increasing the stiffness of the annular ring, the suitable value of natural frequency can be obtained well away from the frequency range of possible perturbations and, consequently, an effective control of vibrational devastation can be achieved. Numerically, the most effective of these parameters studied is stiffness of the annular ring and the least responsive is the second moment of inertia.

10. CONCLUSION

From this study it can be concluded that the system can be made stiffer and resistant to vibrational devastation by making use of the intermediate support. If

the frequency zone of possible perturbations of a system is known, the support tube parameters can be adjusted to mismatch the natural frequency of the system with that of the perturbation and thus the resonance catastrophe can be avoided. By increasing the natural frequency of the system, the net amplitude of the vibrations can be minimized to a reasonable extent along with its quicker damping. Thus, the model developed can work as a suitable tool to assess the optimal values of support tube parameters and hence can help in avoiding vibrational devastation.

ACKNOWLEDGMENTS

The authors are deeply indebted to Dr A. Q. Khan, Ch. M. Ashraf and Dr M. Zubair Khan for their continuous support, encouragement and computational facilities which made this work possible. Thanks are also due to Dr M. Ashraf Atta and Dr Altaf Hussain for their valuable suggestions and Mian M. Aslam for his help in computations.

REFERENCES

1. M. M. Nazeer and M. Afzal 1996 *Proceedings of the* 1*st National Conference on Vibrations in Rotating Machinery*, *NCVRM*-96, 7–9 *September*, *Islamabad*, *Pakistan*, 277–306. Mathematical modeling of fluid flow induced vibrations in centrifuge feed-waste tube-set assembly.
2. M. M. Nazeer 1996 *Proceedings of the* 1*st National Conference on Vibrations in Rotating Machinery*, *NCVRM*-96, 7–9 *September*, *Islamabad*, *Pakistan*, 441–470. Mathematical modeling of magnetic balancing, damping and vibration control.
3. M. M. Nazeer 1997 *Proceedings of the* 1*st National Conference Pakistan*, *Institute of Physics*, *PIP* 97, *Pakistan*, Magnetic balancing, damping and vibration control of resonantly excited system.
4. A. F. Khan, M. K. K. Ghauri, R. H. Shah, A. Hussain and M. A. Atta 1996 *Proceedings of the* 1*st National Conference on Vibrations in Rotating Machinery*, *NCVRM*-96, 7–9 *September*, *Islamabad*, *Pakistan*, 535–544. Damping effect due to difference in natural frequencies in a multibody dynamic system with annular clearance.
5. M. M. Nazeer, M. Afzal, A. F. Khan and N. Ahmed 1998 *International Journal of Computer and Mathematics with Applications*, *USA* **36**, 15–127. Mathematical modeling and computer simulation of two orthogonally forced transverse vibrations in multisegment hanging cantilever.
6. M. M. Nazeer, M. Afzal, A. F. Khan and N. Ahmed 1999 *Journal of Computer Methods in Applied Mechanics and Engineering*. Mathematical modeling and computer simulation of loose spring skirt damping and control of vibrations in a multisegment hanging cantilever (to appear).
7. M. M. Nazeer, A. F. Khan, N. Ahmed and M. Afzal 1997 *Proceedings of the* 6*th All Pakistan Science Conference*, 3–6 *November*, *Peshawar*, *Pakistan*. Loose spring skirt clearance effect on damping and control of vibrations in a multi segment hanging cantilever.
8. A. F. Khan, M. M. Nazeer, R. H. Shah, M. Afzal and N. Ahmed 1997 *Proceedings of the* 6*th National Symposium on Frontiers in Physics*, 16–18 *December*, *Islamabad*, *Pakistan*. Loose spring skirt mounting position effect on damping and control of vibrations in a multi segment hanging cantilever.
9. M. M. Nazeer, A. F. Khan, M. Afzal, N. Ahmed and R. H. Shah 1997 *Proceedings of the* 6*th National Symposium on Frontiers in Physics*, 16–18 *December*, *Islamabad*, *Pakistan*. Study and analysis of loose spring skirt length effect on damping and control of vibrations in a hanging cantilever.

10. W. G. Green 1963 *Theory of Machines*. London, Blackie & Sons Ltd. 1973, re-issue by NBFP.
11. G. H. Ryder 1975 *Strength of Material*. London: English Language Book Society and McMillan Press Ltd.
12. S. Timoshenko 1978 *Strength of Material—Part I. Elementary*. New York: Van Nostrand Reinhold Company.
13. W. T. Thomson 1973 *Vibration Theory and Applications*, London: George Allen & Unwin Ltd.
14. M. L. James, G. M. Smith, J. C. Wolford and P. W. Whaley 1993 *Vibration of Mechanical and Structural Systems with Microcomputer Applications*. New York: Harper Collins College Publishers, second edition.
15. A. L. Kimball 1929 *Transactions of ASME, APM* 21–51. Vibration damping including the case of solid damping.
16. L. Lapidus 1962 *Digital Computation for Chemical Engineers*, U.S.A: McGraw-Hill.
17. M. M. Nazeer, M. Afzal, G. F. Tariq and N. Ahmed 1998 *International Journal of Computer and Mathematics with Applications, USA* **36**, 63–76. Mathematical modeling and computer simulation of transient flow in centrifuge cascade pipe network with optimizing techniques.
18. S. S. Rao 1984 *Mechanical Vibrations*, Reading, MA: Addison-Wesley, second edition.